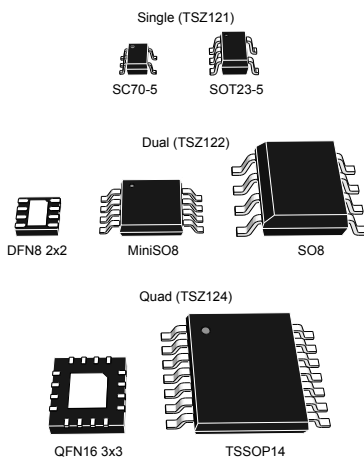


Very high accuracy (5 μ V) zero drift micropower 5 V operational amplifiers


Features

- Very high accuracy and stability: offset voltage 5 μ V max at 25 °C, 8 μ V over full temperature range (-40 °C to 125 °C)
- Rail-to-rail input and output
- Low supply voltage: 1.8 - 5.5 V
- Low power consumption: 40 μ A max. at 5 V
- Gain bandwidth product: 400 kHz
- High tolerance to ESD: 4 kV HBM
- Extended temperature range: -40 to 125 °C
- Micro-packages: SC70-5, DFN8 2x2, and QFN16 3x3

Applications

- Battery-powered applications
- Portable devices
- Signal conditioning
- Medical instrumentation

Description

The TSZ12x series of high precision operational amplifiers offer very low input offset voltages with virtually zero drift.

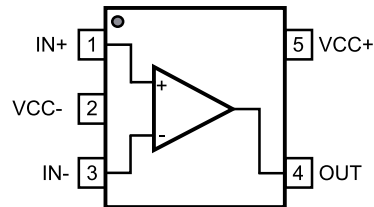
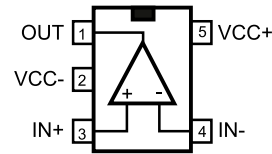
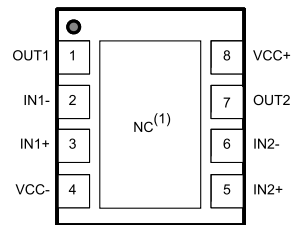
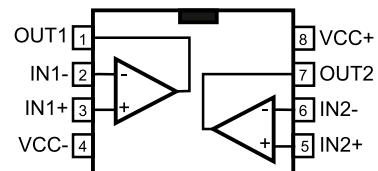
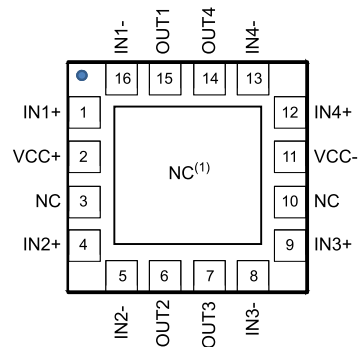
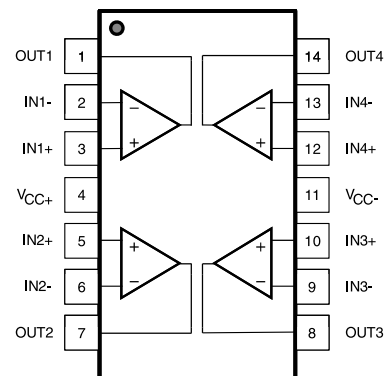
TSZ121 is the single version, **TSZ122** the dual version, and **TSZ124** the quad version, with pinouts compatible with industry standards.

The TSZ12x series offers rail-to-rail input and output, excellent speed/power consumption ratio, and 400 kHz gain bandwidth product, while consuming less than 40 μ A at 5 V. The devices also feature an ultra-low input bias current.

These features make the TSZ12x family ideal for sensor interfaces, battery-powered applications and portable applications.

Maturity status link	
TSZ121	
TSZ122	
TSZ124	
Related products	
TSV711	Continuous-time precision amplifiers
TSV731	
Benefits	
Higher accuracy without calibration	
Accuracy virtually unaffected by temperature change	

1 Package pin connections

Figure 1. Pin connections for each package (top view)

SC70-5

SOT23-5

DFN8 2x2

MiniSO8 and SO8

QFN16 3x3

TSSOP14

1. The exposed pads of the DFN8 2x2 and the QFN16 3x3 can be connected to VCC- or left floating.

2 Absolute maximum ratings and operating conditions

Table 1. Absolute maximum ratings (AMR)

Symbol	Parameter	Value	Unit	
V_{CC}	Supply voltage ⁽¹⁾	6	V	
V_{id}	Differential input voltage ⁽²⁾	$\pm V_{CC}$		
V_{in}	Input voltage ⁽³⁾	$(V_{CC-}) - 0.2$ to $(V_{CC+}) + 0.2$		
I_{in}	Input current ⁽⁴⁾	10	mA	
T_{stg}	Storage temperature	-65 to 150	°C	
T_j	Maximum junction temperature	150		
R_{thja}	Thermal resistance junction to ambient ^{(5) (6)}	SC70-5	205	°C/W
		SOT23-5	250	
		DFN8 2x2	57	
		MiniSO8	190	
		SO8	125	
		QFN16 3x3	39	
		TSSOP14	100	
ESD	HBM: human body model ⁽⁷⁾	4	kV	
	MM: machine model ⁽⁸⁾	300	V	
	CDM: charged device model ⁽⁹⁾	1.5	kV	
	Latch-up immunity	200	mA	

1. All voltage values, except the differential voltage are with respect to the network ground terminal.
2. The differential voltage is the non-inverting input terminal with respect to the inverting input terminal.
3. $V_{CC} - V_{in}$ must not exceed 6 V, V_{in} must not exceed 6 V
4. Input current must be limited by a resistor in series with the inputs.
5. R_{th} are typical values.
6. Short-circuits can cause excessive heating and destructive dissipation.
7. Human body model: 100 pF discharged through a 1.5 kΩ resistor between two pins of the device, done for all couples of pin combinations with other pins floating.
8. Machine model: a 200 pF cap is charged to the specified voltage, then discharged directly between two pins of the device with no external series resistor (internal resistor < 5 Ω), done for all couples of pin combinations with other pins floating.
9. Charged device model: all pins plus package are charged together to the specified voltage and then discharged directly to ground.

Table 2. Operating conditions

Symbol	Parameter	Value	Unit
V_{CC}	Supply voltage	1.8 to 5.5	V
V_{icm}	Common mode input voltage range	$(V_{CC-}) - 0.1$ to $(V_{CC+}) + 0.1$	
T_{oper}	Operating free air temperature range	-40 to 125	°C

3 Electrical characteristics

Table 3. Electrical characteristics at $V_{CC+} = 1.8\text{ V}$ with $V_{CC-} = 0\text{ V}$, $V_{icm} = V_{CC}/2$, $T = 25\text{ }^{\circ}\text{C}$, and $R_L = 10\text{ k}\Omega$ connected to $V_{CC}/2$ (unless otherwise specified)

Symbol	Parameter	Conditions	Min.	Typ.	Max.	Unit
DC performance						
V_{io}	Input offset voltage	$T = 25\text{ }^{\circ}\text{C}$		1	5	μV
		$-40\text{ }^{\circ}\text{C} < T < 125\text{ }^{\circ}\text{C}$			8	
$\Delta V_{io}/\Delta T$	Input offset voltage drift ⁽¹⁾	$-40\text{ }^{\circ}\text{C} < T < 125\text{ }^{\circ}\text{C}$		10	30	$\text{nV}/^{\circ}\text{C}$
I_{ib}	Input bias current ($V_{out} = V_{CC}/2$)	$T = 25\text{ }^{\circ}\text{C}$		50	200 ⁽²⁾	pA
		$-40\text{ }^{\circ}\text{C} < T < 125\text{ }^{\circ}\text{C}$			300 ⁽²⁾	
I_{io}	Input offset current ($V_{out} = V_{CC}/2$)	$T = 25\text{ }^{\circ}\text{C}$		100	400 ⁽²⁾	pA
		$-40\text{ }^{\circ}\text{C} < T < 125\text{ }^{\circ}\text{C}$			600 ⁽²⁾	
CMR	Common mode rejection ratio, $20 \log(\Delta V_{icm}/\Delta V_{io})$, $V_{ic} = 0\text{ V}$ to V_{CC} , $V_{out} = V_{CC}/2$, $R_L > 1\text{ M}\Omega$	$T = 25\text{ }^{\circ}\text{C}$	110	122		dB
		$-40\text{ }^{\circ}\text{C} < T < 125\text{ }^{\circ}\text{C}$	110			
A_{vd}	Large signal voltage gain, $V_{out} = 0.5\text{ V}$ to $(V_{CC} - 0.5\text{ V})$	$T = 25\text{ }^{\circ}\text{C}$	118	135		dB
		$-40\text{ }^{\circ}\text{C} < T < 125\text{ }^{\circ}\text{C}$	110			
V_{OH}	High-level output voltage	$T = 25\text{ }^{\circ}\text{C}$			30	mV
		$-40\text{ }^{\circ}\text{C} < T < 125\text{ }^{\circ}\text{C}$			70	
V_{OL}	Low-level output voltage	$T = 25\text{ }^{\circ}\text{C}$			30	mV
		$-40\text{ }^{\circ}\text{C} < T < 125\text{ }^{\circ}\text{C}$			70	
I_{out}	I_{sink} ($V_{out} = V_{CC}$)	$T = 25\text{ }^{\circ}\text{C}$	7	8		mA
		$-40\text{ }^{\circ}\text{C} < T < 125\text{ }^{\circ}\text{C}$	6			
	I_{source} ($V_{out} = 0\text{ V}$)	$T = 25\text{ }^{\circ}\text{C}$	5	7		
		$-40\text{ }^{\circ}\text{C} < T < 125\text{ }^{\circ}\text{C}$	4			
I_{CC}	Supply current (per amplifier, $V_{out} = V_{CC}/2$, $R_L > 1\text{ M}\Omega$)	$T = 25\text{ }^{\circ}\text{C}$		28	40	μA
		$-40\text{ }^{\circ}\text{C} < T < 125\text{ }^{\circ}\text{C}$			40	
AC performance						
GBP	Gain bandwidth product	$R_L = 10\text{ k}\Omega$, $C_L = 100\text{ pF}$		400		kHz
F_u	Unity gain frequency			300		
ϕ_m	Phase margin			55		Degrees
G_m	Gain margin			17		dB
SR	Slew rate ⁽³⁾			0.17		$\text{V}/\mu\text{s}$
t_s	Setting time		To 0.1%, $V_{in} = 1\text{ Vp-p}$, $R_L = 10\text{ k}\Omega$, $C_L = 100\text{ pF}$		50	
e_n	Equivalent input noise voltage	$f = 1\text{ kHz}$		60		$\text{nV}/\sqrt{\text{Hz}}$
		$f = 10\text{ kHz}$		60		
$\int e_n$	Low-frequency peak-to-peak input noise	Bandwidth, $f = 0.1$ to 10 Hz		1.1		μVpp
C_s	Channel separation	$f = 100\text{ Hz}$		120		dB

Symbol	Parameter	Conditions	Min.	Typ.	Max.	Unit
t_{init}	Initialization time	T = 25 °C		50		μs
		-40 °C < T < 125 °C		100		

1. See Section 5.5 *Input offset voltage drift over temperature*. Input offset measurements are performed on $\times 100$ gain configuration. The amplifiers and the gain setting resistors are at the same temperature.
2. Guaranteed by design
3. Slew rate value is calculated as the average between positive and negative slew rates.

Table 4. Electrical characteristics at $V_{CC+} = 3.3\text{ V}$ with $V_{CC-} = 0\text{ V}$, $V_{icm} = V_{CC}/2$, T = 25 °C, and $R_L = 10\text{ k}\Omega$ connected to $V_{CC}/2$ (unless otherwise specified)

Symbol	Parameter	Conditions	Min.	Typ.	Max.	Unit
DC performance						
V_{io}	Input offset voltage	T = 25 °C		1	5	μV
		-40 °C < T < 125 °C			8	
$\Delta V_{io}/\Delta T$	Input offset voltage drift ⁽¹⁾	-40 °C < T < 125 °C		10	30	nV/°C
I_{ib}	Input bias current ($V_{out} = V_{CC}/2$)	T = 25 °C		60	200 ⁽²⁾	pA
		-40 °C < T < 125 °C			300 ⁽²⁾	
I_{io}	Input offset current ($V_{out} = V_{CC}/2$)	T = 25 °C		120	400 ⁽²⁾	pA
		-40 °C < T < 125 °C			600 ⁽²⁾	
CMR	Common mode rejection ratio, 20 log ($\Delta V_{icm}/\Delta V_{io}$), $V_{ic} = 0\text{ V}$ to V_{CC} , $V_{out} = V_{CC}/2$, $R_L > 1\text{ M}\Omega$	T = 25 °C	115	128		dB
		-40 °C < T < 125 °C	115			
A_{vd}	Large signal voltage gain, $V_{out} = 0.5\text{ V}$ to $(V_{CC} - 0.5\text{ V})$	T = 25 °C	118	135		dB
		-40 °C < T < 125 °C	110			
V_{OH}	High-level output voltage	T = 25 °C			30	mV
		-40 °C < T < 125 °C			70	
V_{OL}	Low-level output voltage	T = 25 °C			30	mV
		-40 °C < T < 125 °C			70	
I_{out}	I_{sink} ($V_{out} = V_{CC}$)	T = 25 °C	15	18		mA
		-40 °C < T < 125 °C	12			
	I_{source} ($V_{out} = 0\text{ V}$)	T = 25 °C	14	16		
		-40 °C < T < 125 °C	10			
I_{CC}	Supply current (per amplifier, $V_{out} = V_{CC}/2$, $R_L > 1\text{ M}\Omega$)	T = 25 °C		29	40	μA
		-40 °C < T < 125 °C			40	
AC performance						
GBP	Gain bandwidth product	$R_L = 10\text{ k}\Omega$, $C_L = 100\text{ pF}$		400		kHz
F_u	Unity gain frequency			300		
ϕ_m	Phase margin			56		Degrees
G_m	Gain margin			19		dB
SR	Slew rate ⁽³⁾			0.19		V/ μs
t_s	Setting time		To 0.1 %, $V_{in} = 1\text{ V}_{p-p}$, $R_L = 10\text{ k}\Omega$, $C_L = 100\text{ pF}$		50	

Symbol	Parameter	Conditions	Min.	Typ.	Max.	Unit
e_n	Equivalent input noise voltage	f = 1 kHz		40		nV/ $\sqrt{\text{Hz}}$
		f = 10 kHz		40		
$\int e_n$	Low-frequency peak-to-peak input noise	Bandwidth, f = 0.1 to 10 Hz		0.8		μVpp
C_s	Channel separation	f = 100 Hz		120		dB
t_{init}	Initialization time	T = 25 °C		50		μs
		-40 °C < T < 125 °C		100		

1. See [Section 5.5 Input offset voltage drift over temperature](#). Input offset measurements are performed on $\times 100$ gain configuration. The amplifiers and the gain setting resistors are at the same temperature.
2. Guaranteed by design
3. Slew rate value is calculated as the average between positive and negative slew rates.

Table 5. Electrical characteristics at $V_{CC+} = 5\text{ V}$ with $V_{CC-} = 0\text{ V}$, $V_{\text{icm}} = V_{CC}/2$, T = 25 °C, and $R_L = 10\text{ k}\Omega$ connected to $V_{CC}/2$ (unless otherwise specified)

Symbol	Parameter	Conditions	Min.	Typ.	Max.	Unit
DC performance						
V_{io}	Input offset voltage	T = 25 °C		1	5	μV
		-40 °C < T < 125 °C			8	
$\Delta V_{\text{io}}/\Delta T$	Input offset voltage drift ⁽¹⁾	-40 °C < T < 125 °C		10	30	nV/°C
I_{ib}	Input bias current ($V_{\text{out}} = V_{CC}/2$)	T = 25 °C		70	200 ⁽²⁾	pA
		-40 °C < T < 125 °C			300 ⁽²⁾	
I_{io}	Input offset current ($V_{\text{out}} = V_{CC}/2$)	T = 25 °C		140	400 ⁽²⁾	pA
		-40 °C < T < 125 °C			600 ⁽²⁾	
CMR	Common mode rejection ratio, 20 log ($\Delta V_{\text{icm}}/\Delta V_{\text{io}}$), $V_{\text{ic}} = 0\text{ V}$ to V_{CC} , $V_{\text{out}} = V_{CC}/2$, $R_L > 1\text{ M}\Omega$	T = 25 °C	115	136		dB
		-40 °C < T < 125 °C	115			
SVR	Supply voltage rejection ratio, 20 log ($\Delta V_{CC}/\Delta V_{\text{io}}$), $V_{CC} = 1.8\text{ V}$ to 5.5 V , $V_{\text{out}} = V_{CC}/2$, $R_L > 1\text{ M}\Omega$	T = 25 °C	120	140		dB
		-40 °C < T < 125 °C	120			
A_{vd}	Large signal voltage gain, $V_{\text{out}} = 0.5\text{ V}$ to $(V_{CC} - 0.5\text{ V})$	T = 25 °C	120	135		dB
		-40 °C < T < 125 °C	110			
EMIRR ⁽³⁾	EMI rejection rate = -20 log ($V_{\text{RFpeak}}/\Delta V_{\text{io}}$)	$V_{\text{RF}} = 100\text{ mVp}$, f = 400 MHz		84		dB
		$V_{\text{RF}} = 100\text{ mVp}$, f = 900 MHz		87		
		$V_{\text{RF}} = 100\text{ mVp}$, f = 1800 MHz		90		
		$V_{\text{RF}} = 100\text{ mVp}$, f = 2400 MHz		91		
V_{OH}	High-level output voltage	T = 25 °C			30	mV
		-40 °C < T < 125 °C			70	
V_{OL}	Low-level output voltage	T = 25 °C			30	mV
		-40 °C < T < 125 °C			70	

Symbol	Parameter	Conditions	Min.	Typ.	Max.	Unit
I_{out}	$I_{sink} (V_{out} = V_{CC})$	$T = 25\text{ }^{\circ}\text{C}$	15	18		mA
		$-40\text{ }^{\circ}\text{C} < T < 125\text{ }^{\circ}\text{C}$	14			
	$I_{source} (V_{out} = 0\text{ V})$	$T = 25\text{ }^{\circ}\text{C}$	14	17		
		$-40\text{ }^{\circ}\text{C} < T < 125\text{ }^{\circ}\text{C}$	12			
I_{CC}	Supply current (per amplifier, $V_{out} = V_{CC}/2$, $R_L > 1\text{ M}\Omega$)	$T = 25\text{ }^{\circ}\text{C}$		31	40	μA
		$-40\text{ }^{\circ}\text{C} < T < 125\text{ }^{\circ}\text{C}$			40	
AC performance						
GBP	Gain bandwidth product	$R_L = 10\text{ k}\Omega$, $C_L = 100\text{ pF}$		400		kHz
F_u	Unity gain frequency			300		
ϕ_m	Phase margin			53		Degrees
G_m	Gain margin			19		dB
SR	Slew rate ⁽⁴⁾			0.19		V/ μs
t_s	Setting time	To 0.1 %, $V_{in} = 100\text{ mVp-p}$, $R_L = 10\text{ k}\Omega$, $C_L = 100\text{ pF}$		10		μs
e_n	Equivalent input noise voltage	$f = 1\text{ kHz}$		37		nV/ $\sqrt{\text{Hz}}$
		$f = 10\text{ kHz}$		37		
j_{e_n}	Low-frequency peak-to-peak input noise	Bandwidth, $f = 0.1\text{ to }10\text{ Hz}$		0.75		μVpp
C_s	Channel separation	$f = 100\text{ Hz}$		120		dB
t_{init}	Initialization time	$T = 25\text{ }^{\circ}\text{C}$		50		μs
		$-40\text{ }^{\circ}\text{C} < T < 125\text{ }^{\circ}\text{C}$		100		

1. See [Section 5.5 Input offset voltage drift over temperature](#). Input offset measurements are performed on $\times 100$ gain configuration. The amplifiers and the gain setting resistors are at the same temperature.
2. Guaranteed by design
3. Tested on SC70-5 package
4. Slew rate value is calculated as the average between positive and negative slew rates.

4 Electrical characteristic curves

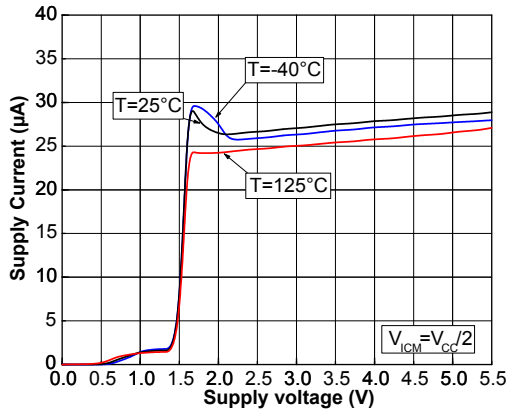
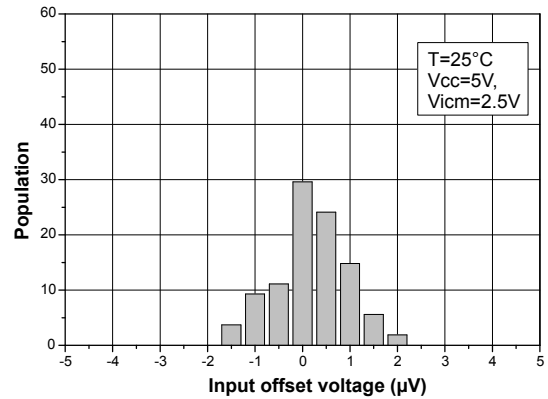
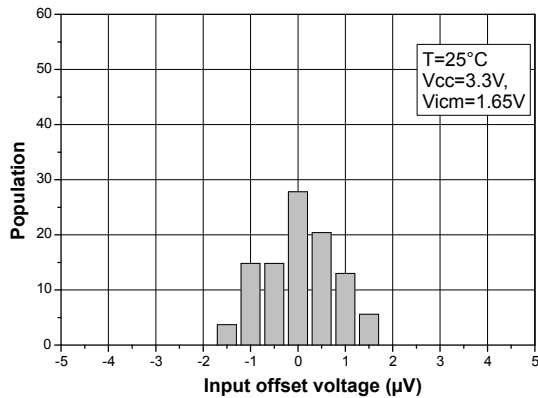
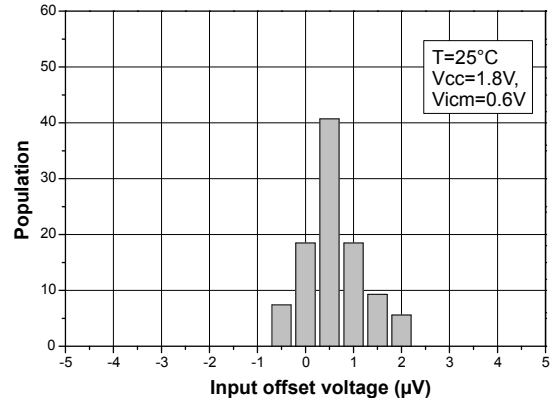
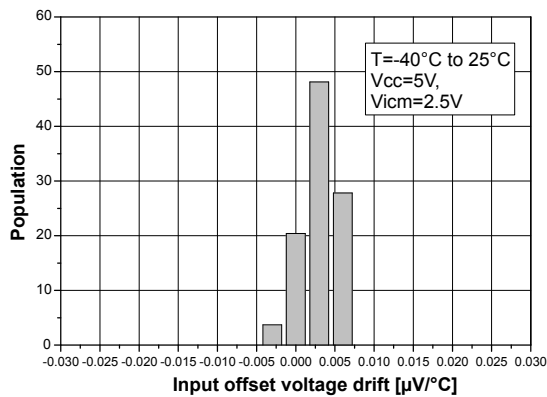
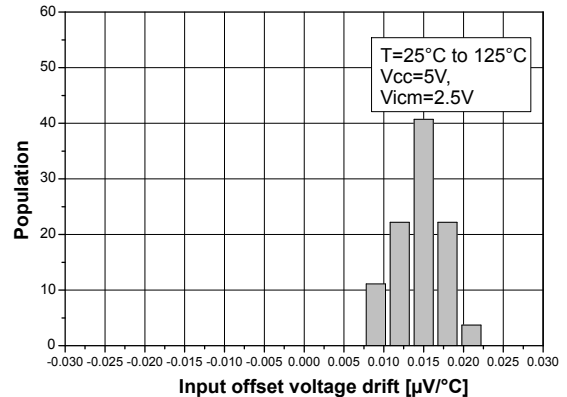
Figure 2. Supply current vs. supply voltage

Figure 3. Input offset voltage distribution at $V_{CC} = 5\text{ V}$

Figure 4. Input offset voltage distribution at $V_{CC} = 3.3\text{ V}$

Figure 5. Input offset voltage distribution at $V_{CC} = 1.8\text{ V}$

Figure 6. Vio temperature co-efficient distribution (-40 °C to 25 °C)

Figure 7. Vio temperature co-efficient distribution (25 °C to 125 °C)


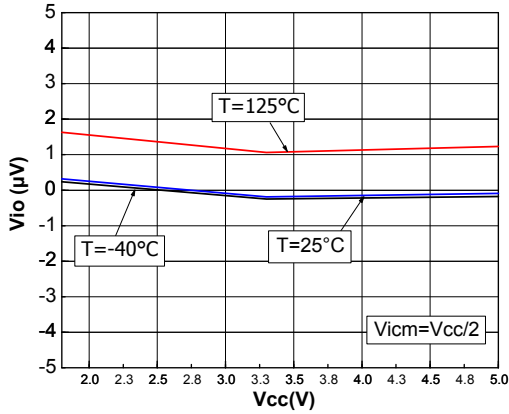
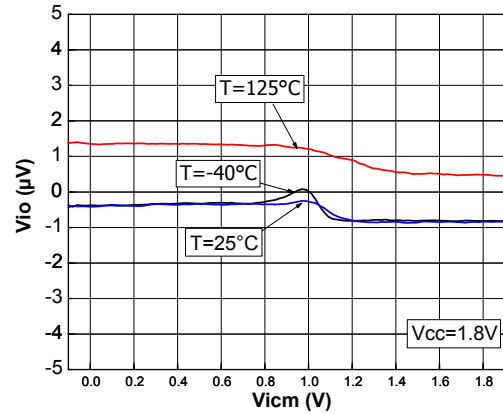
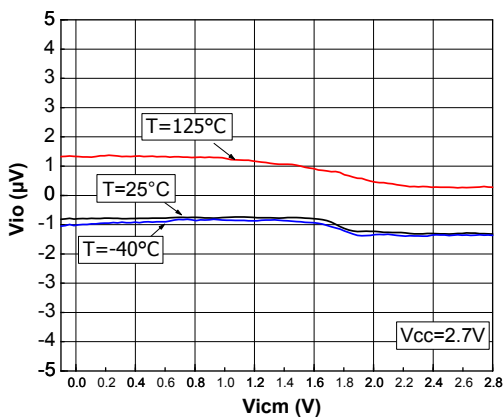
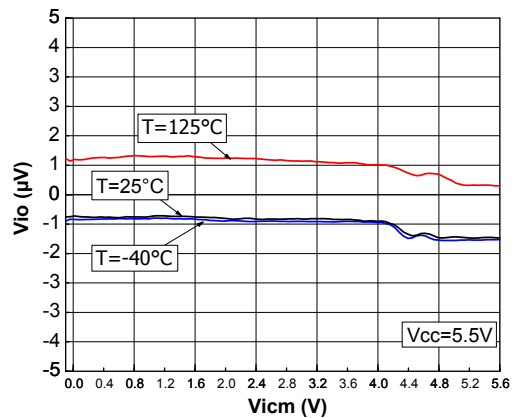
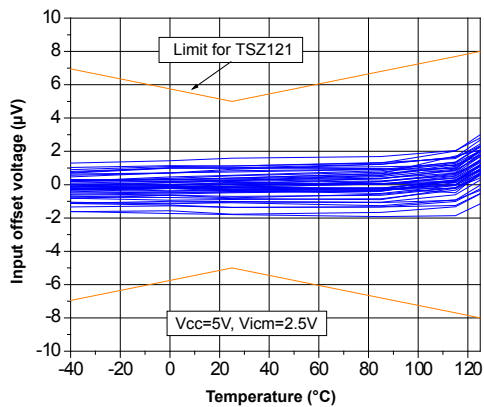
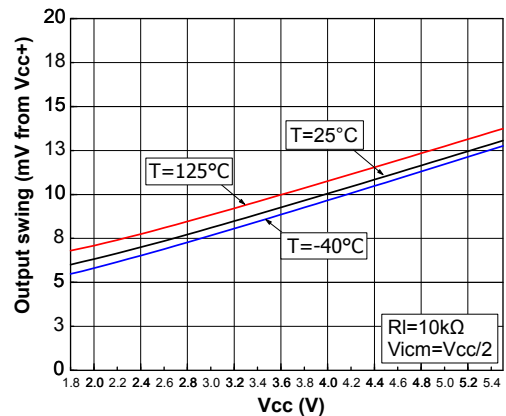
Figure 8. Input offset voltage vs. supply voltage

Figure 9. Input offset voltage vs. input common-mode at $V_{cc} = 1.8\text{ V}$

Figure 10. Input offset voltage vs. input common-mode at $V_{cc} = 2.7\text{ V}$

Figure 11. Input offset voltage vs. input common-mode at $V_{cc} = 5.5\text{ V}$

Figure 12. Input offset voltage vs. temperature

Figure 13. V_{OH} vs. supply voltage


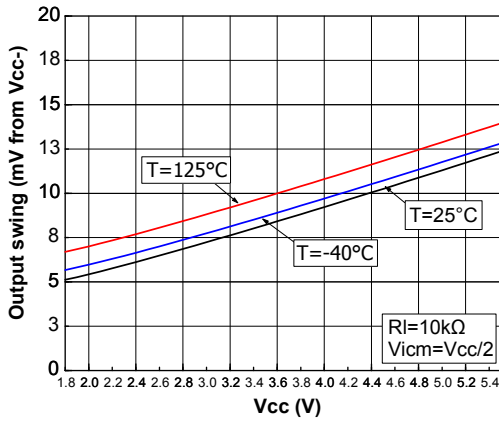
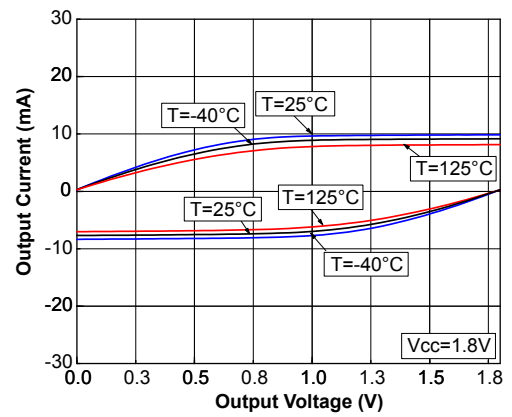
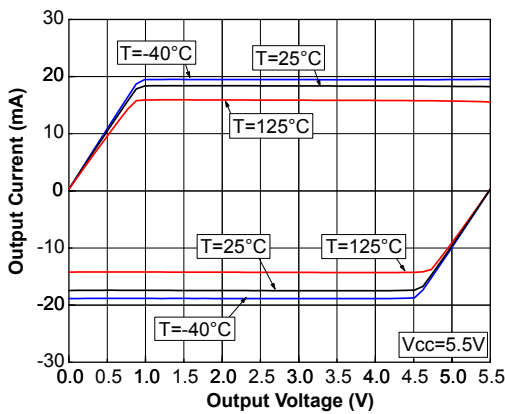
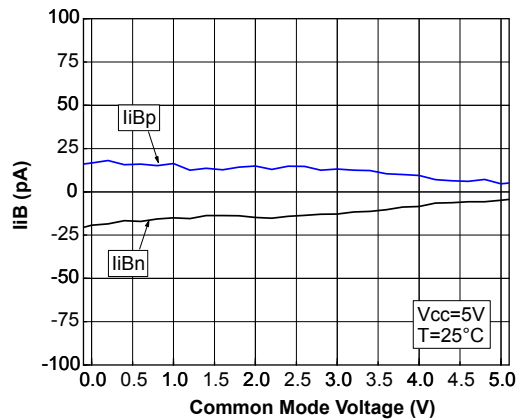
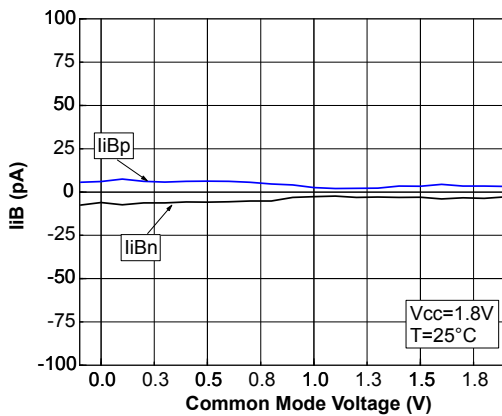
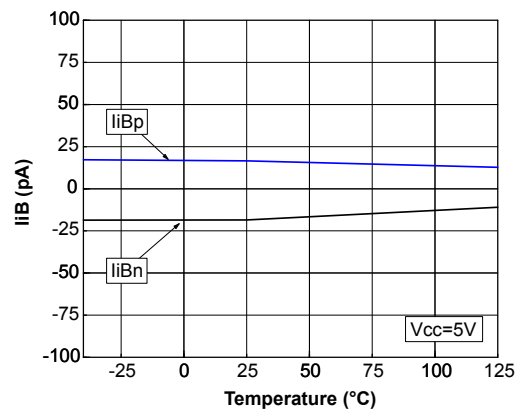
Figure 14. V_{OL} vs. supply voltage

Figure 15. Output current vs. output voltage at $V_{CC} = 1.8\text{ V}$

Figure 16. Output current vs. output voltage at $V_{CC} = 5.5\text{ V}$

Figure 17. Input bias current vs. common mode at $V_{CC} = 5\text{ V}$

Figure 18. Input bias current vs. common mode at $V_{CC} = 1.8\text{ V}$

Figure 19. Input bias current vs. temperature at $V_{CC} = 5\text{ V}$


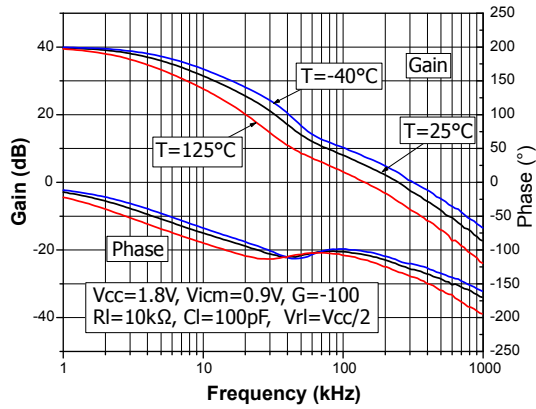
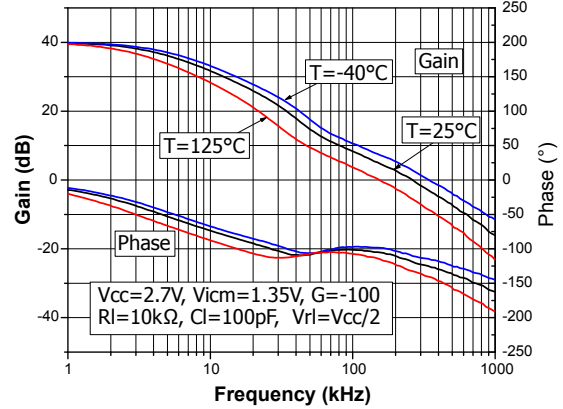
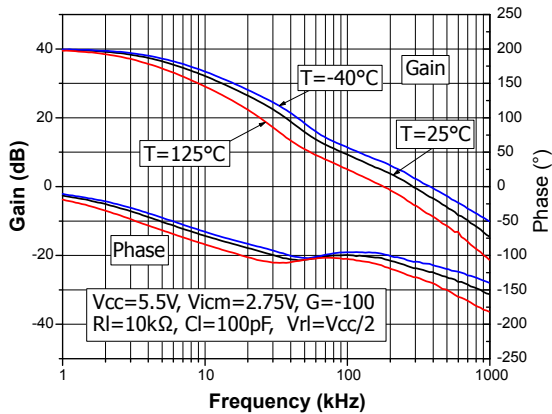
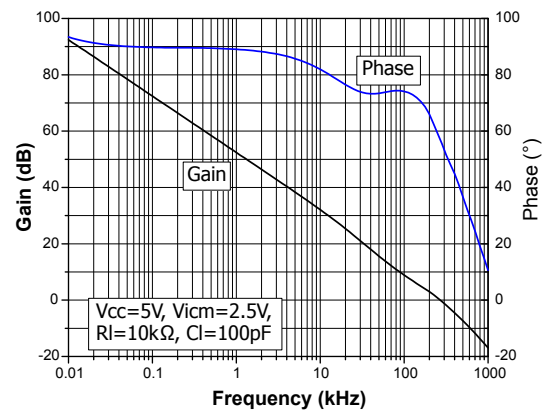
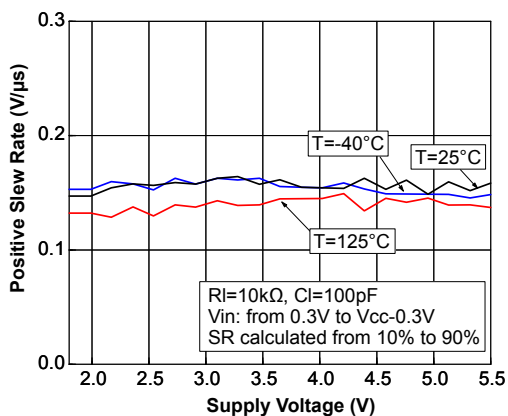
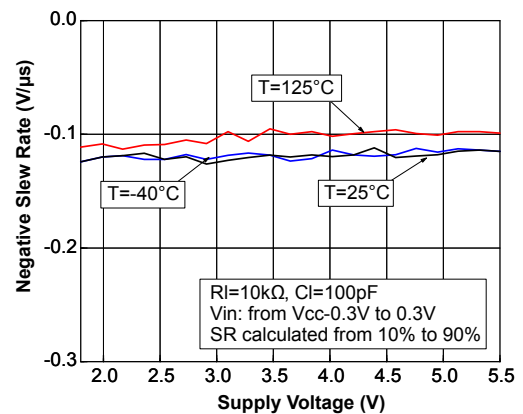
Figure 20. Bode diagram at $V_{CC} = 1.8\text{ V}$

Figure 21. Bode diagram at $V_{CC} = 2.7\text{ V}$

Figure 22. Bode diagram at $V_{CC} = 5.5\text{ V}$

Figure 23. Open loop gain vs. frequency

Figure 24. Positive slew rate vs. supply voltage

Figure 25. Negative slew rate vs. supply voltage


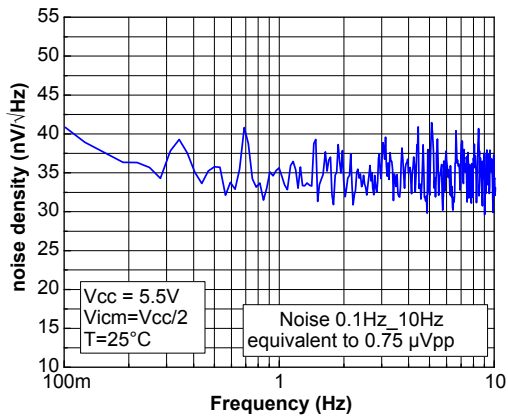
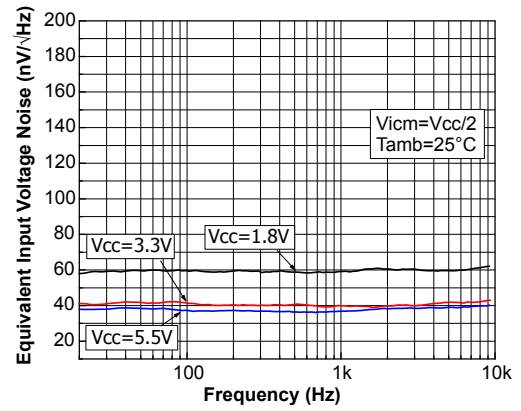
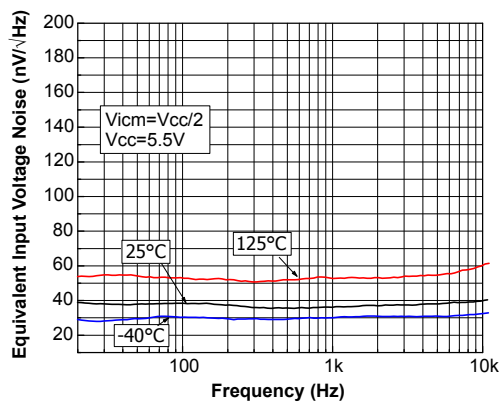
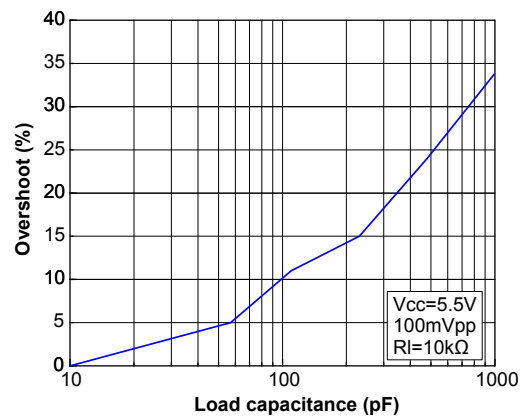
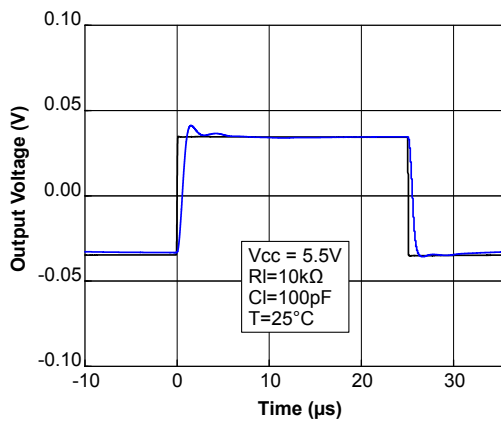
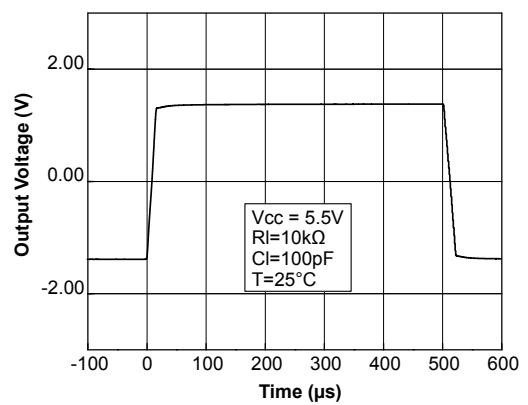
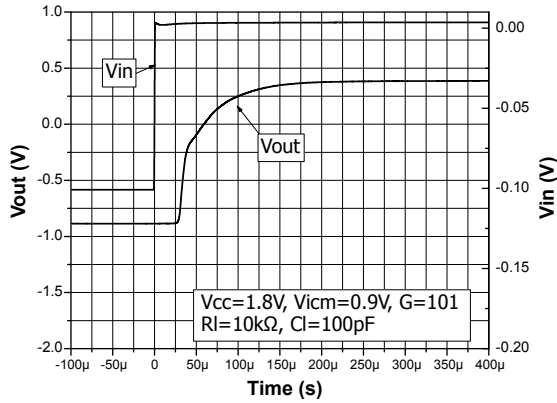
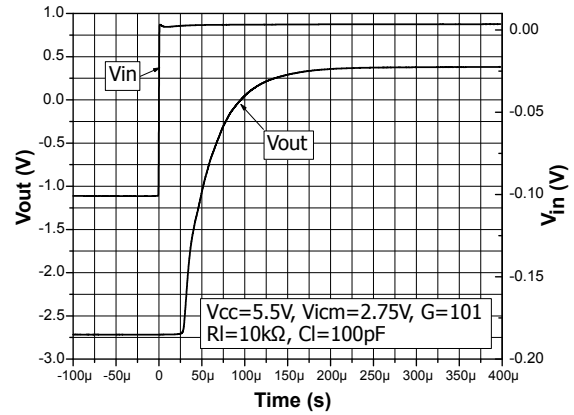
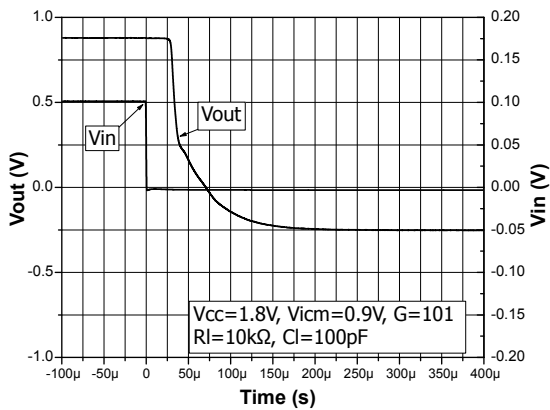
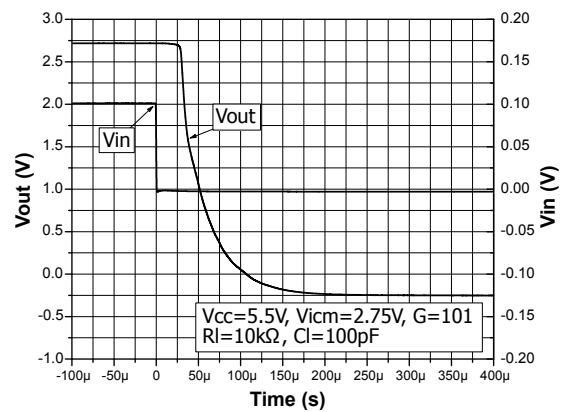
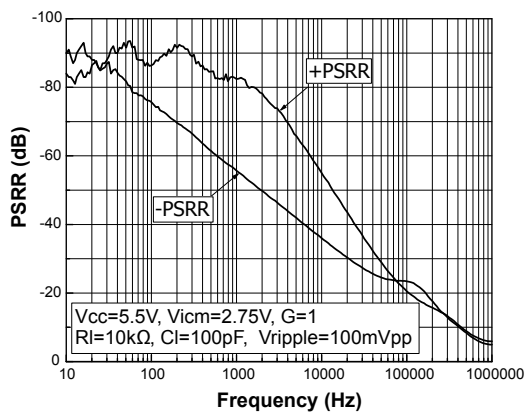
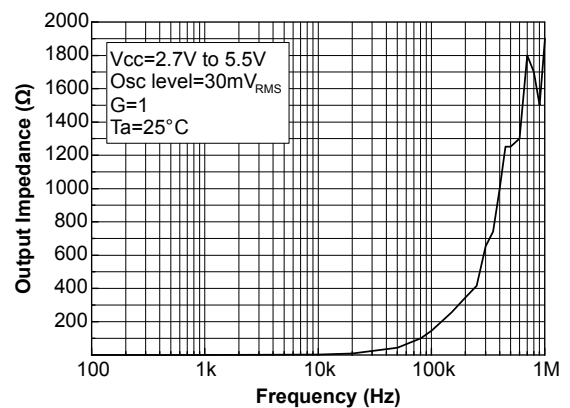
Figure 26. 0.1 Hz to 10 Hz noise

Figure 27. Noise vs. frequency

Figure 28. Noise vs. frequency and temperature

Figure 29. Output overshoot vs. load capacitance

Figure 30. Small signal

Figure 31. Large signal


Figure 32. Positive overvoltage recovery at $V_{CC} = 1.8\text{ V}$

Figure 33. Positive overvoltage recovery at $V_{CC} = 5\text{ V}$

Figure 34. Negative overvoltage recovery at $V_{CC} = 1.8\text{ V}$

Figure 35. Negative overvoltage recovery at $V_{CC} = 5\text{ V}$

Figure 36. PSRR vs. frequency

Figure 37. Output impedance vs. frequency


5 Application information

5.1 Operation theory

The TSZ121, TSZ122, and TSZ124 are high precision CMOS devices. They achieve a low offset drift and no $1/f$ noise thanks to their chopper architecture. Chopper-stabilized amps constantly correct low-frequency errors across the inputs of the amplifier.

Chopper-stabilized amplifiers can be explained with respect to:

- Time domain
- Frequency domain

5.1.1 Time domain

The basis of the chopper amplifier is realized in two steps. These steps are synchronized thanks to a clock running at 400 kHz.

Figure 38. Block diagram in the time domain (step 1)

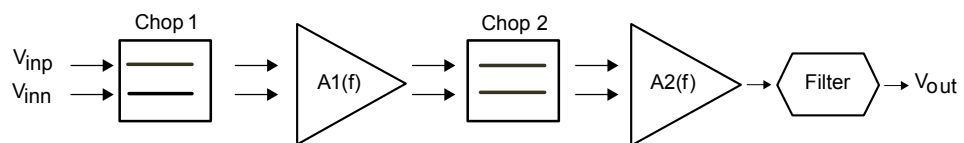


Figure 39. Block diagram in the time domain (step 2)

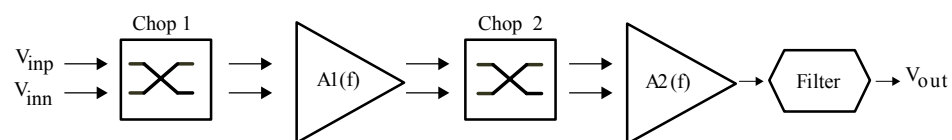


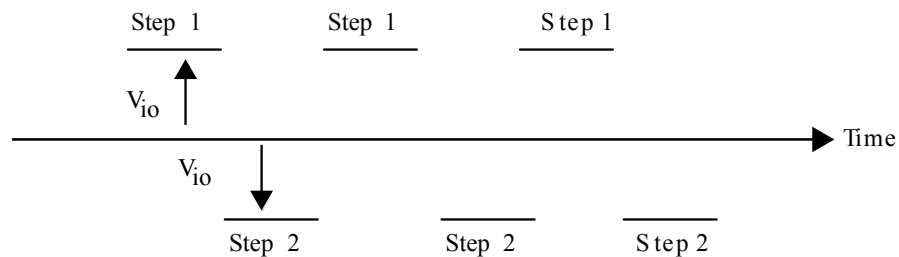
Figure 38. Block diagram in the time domain (step 1) shows step 1, the first clock cycle, where V_{io} is amplified in the normal way.

Figure 39. Block diagram in the time domain (step 2) shows step 2, the second clock cycle, where Chop1 and Chop2 swap paths. At this time, the V_{io} is amplified in a reverse way as compared to step 1.

At the end of these two steps, the average V_{io} is close to zero.

The $A2(f)$ amplifier has a small impact on the V_{io} because the V_{io} is expressed as the input offset and is consequently divided by $A1(f)$.

In the time domain, the offset part of the output signal before filtering is shown in Figure 40. [V_{io} cancellation principle](#).

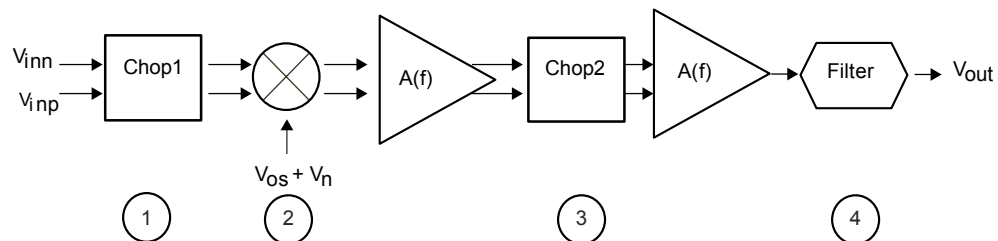
Figure 40. V_{io} cancellation principle


The low pass filter averages the output value resulting in the cancellation of the V_{io} offset.

The $1/f$ noise can be considered as an offset in low frequency and it is canceled like the V_{io} , thanks to the chopper technique.

5.1.2 Frequency domain

The frequency domain gives a more accurate vision of chopper-stabilized amplifier architecture.

Figure 41. Block diagram in the frequency domain


The modulation technique transposes the signal to a higher frequency where there is no $1/f$ noise, and demodulate it back after amplification.

1. According to [Figure 41. Block diagram in the frequency domain](#), the input signal V_{in} is modulated once (Chop1) so all the input signal is transposed to the high frequency domain.
2. The amplifier adds its own error (V_{io} (output offset voltage) + the noise V_n ($1/f$ noise)) to this modulated signal.
3. This signal is then demodulated (Chop2), but since the noise and the offset are modulated only once, they are transposed to the high frequency, leaving the output signal of the amplifier without any offset and low frequency noise. Consequently, the input signal is amplified with a very low offset and $1/f$ noise.
4. To get rid of the high frequency part of the output signal (which is useless) a low pass filter is implemented. To further suppress the remaining ripple down to a desired level, another low pass filter may be added externally on the output of the TSZ121, TSZ122, or TSZ124 device.

5.2 Operating voltages

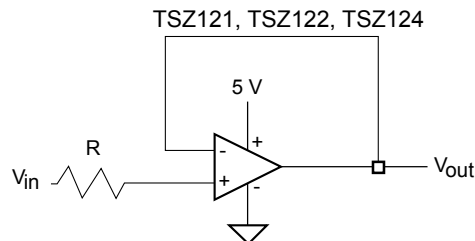
TSZ121, TSZ122, and TSZ124 devices can operate from 1.8 to 5.5 V. The parameters are fully specified for 1.8 V, 3.3 V, and 5 V power supplies. However, the parameters are very stable in the full V_{CC} range and several characterization curves show the TSZ121, TSZ122, and TSZ124 device characteristics at 1.8 V and 5.5 V. Additionally, the main specifications are guaranteed in extended temperature ranges from -40 to 125 °C.

5.3 Input pin voltage ranges

TSZ121, TSZ122, and TSZ124 devices have internal ESD diode protection on the inputs. These diodes are connected between the input and each supply rail to protect the input MOSFETs from electrical discharge. If the input pin voltage exceeds the power supply by 0.5 V, the ESD diodes become conductive and excessive current can flow through them. Without limitation this over current can damage the device.

In this case, it is important to limit the current to 10 mA, by adding resistance on the input pin, as described in Figure 42. Input current limitation.

Figure 42. Input current limitation



5.4 Rail-to-rail input

TSZ121, TSZ122, and TSZ124 devices have a rail-to-rail input, and the input common mode range is extended from $(V_{CC-}) - 0.1\text{ V}$ to $(V_{CC+}) + 0.1\text{ V}$.

5.5 Input offset voltage drift over temperature

The maximum input voltage drift variation over temperature is defined as the offset variation related to the offset value measured at 25 °C. The operational amplifier is one of the main circuits of the signal conditioning chain, and the amplifier input offset is a major contributor to the chain accuracy. The signal chain accuracy at 25 °C can be compensated during production at application level. The maximum input voltage drift over temperature enables the system designer to anticipate the effect of temperature variations.

The maximum input voltage drift over temperature is computed using Equation 1.

Equation 1

$$\frac{\Delta V_{io}}{\Delta T} = \max \left| \frac{V_{io}(T) - V_{io}(25\text{ °C})}{T - 25\text{ °C}} \right|$$

Where $T = -40\text{ °C}$ and 125 °C .

The TSZ121, TSZ122, and TSZ124 datasheet maximum value is guaranteed by measurements on a representative sample size ensuring a C_{pk} (process capability index) greater than 1.3.

5.6 Rail-to-rail output

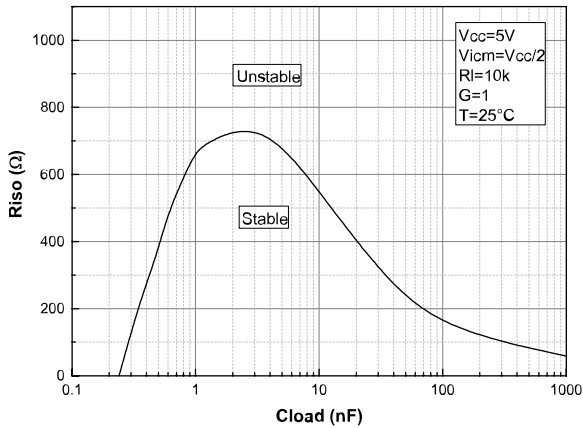
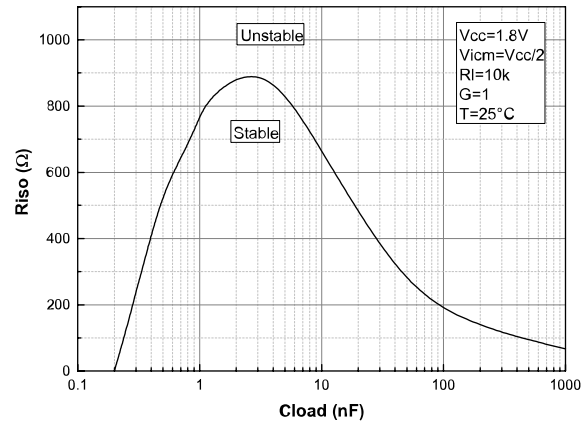
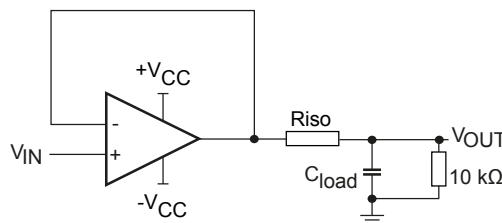
The operational amplifier output levels can go close to the rails: to a maximum of 30 mV above and below the rail when connected to a 10 kΩ resistive load to $V_{CC}/2$.

5.7 Capacitive load

Driving large capacitive loads can cause stability problems. Increasing the load capacitance produces gain peaking in the frequency response, with overshoot and ringing in the step response. It is usually considered that with a gain peaking higher than 2.3 dB an op amp might become unstable.

Generally, the unity gain configuration is the worst case for stability and the ability to drive large capacitive loads.

Figure 43. Stability criteria with a serial resistor at $V_{DD} = 5\text{ V}$ and Figure 44. Stability criteria with a serial resistor at $V_{DD} = 1.8\text{ V}$ show the serial resistor that must be added to the output, to make a system stable. Figure 45. Test configuration for Riso shows the test configuration using an isolation resistor, Riso.

Figure 43. Stability criteria with a serial resistor at $V_{DD} = 5\text{ V}$

Figure 44. Stability criteria with a serial resistor at $V_{DD} = 1.8\text{ V}$

Figure 45. Test configuration for Riso


5.8 PCB layout recommendations

Particular attention must be paid to the layout of the PCB, tracks connected to the amplifier, load, and power supply. The power and ground traces are critical as they must provide adequate energy and grounding for all circuits. Good practice is to use short and wide PCB traces to minimize voltage drops and parasitic inductance.

In addition, to minimize parasitic impedance over the entire surface, a multi-via technique that connects the bottom and top layer ground planes together in many locations is often used.

The copper traces that connect the output pins to the load and supply pins should be as wide as possible to minimize trace resistance.

5.9 Optimized application recommendation

TSZ121, TSZ122, and TSZ124 devices are based on chopper architecture. As they are switched devices, it is strongly recommended to place a $0.1\ \mu\text{F}$ capacitor as close as possible to the supply pins.

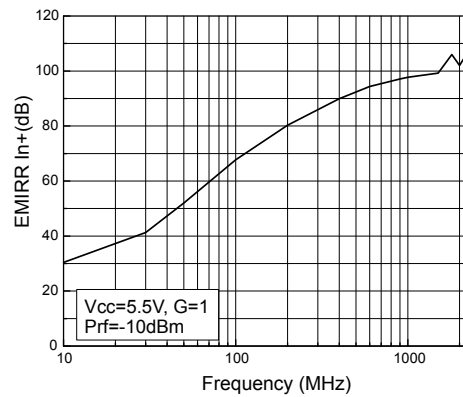
A good decoupling has several advantages for an application. First, it helps to reduce electromagnetic interference. Due to the modulation of the chopper, the decoupling capacitance also helps to reject the small ripple that may appear on the output.

TSZ121, TSZ122, and TSZ124 devices have been optimized for use with $10\ \text{k}\Omega$ in the feedback loop. With this, or a higher value of resistance, these devices offer the best performance.

5.10 EMI rejection ration (EMIRR)

The electromagnetic interference (EMI) rejection ratio, or EMIRR, describes the EMI immunity of operational amplifiers. An adverse effect that is common to many op amps is a change in the offset voltage as a result of RF signal rectification.

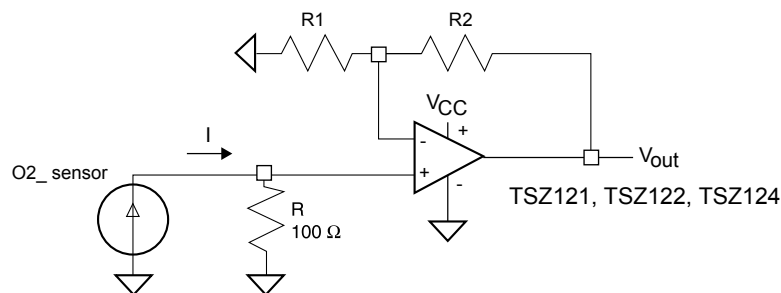
The TSZ121, TSZ122, and TSZ124 have been specially designed to minimize susceptibility to EMIRR and show an extremely good sensitivity. [Figure 46. EMIRR on IN+ pin](#) shows the EMIRR IN+ of the TSZ121, TSZ122, and TSZ124 measured from $10\ \text{MHz}$ up to $2.4\ \text{GHz}$.

Figure 46. EMIRR on IN+ pin


5.11 Application examples

5.11.1 Oxygen sensor

The electrochemical sensor creates a current proportional to the concentration of the gas being measured. This current is converted into voltage thanks to R resistance. This voltage is then amplified by TSZ121, TSZ122, and TSZ124 devices (see [Figure 47. Oxygen sensor principle schematic](#)).

Figure 47. Oxygen sensor principle schematic


The output voltage is calculated using [Equation 2](#):

Equation 2

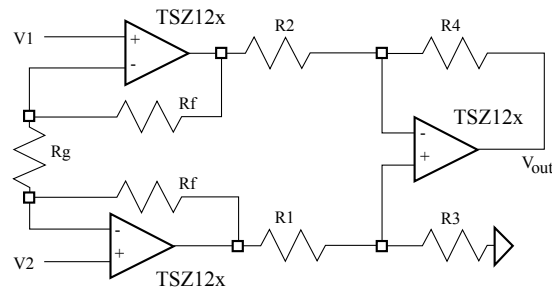
$$V_{out} = (I \times R - V_{io}) \times \left(\frac{R_2}{R_1} + 1 \right)$$

As the current delivered by the O2 sensor is extremely low, the impact of the V_{io} can become significant with a traditional operational amplifier. The use of the chopper amplifier of the TSZ121, TSZ122, or TSZ124 is perfect for this application.

In addition, using TSZ121, TSZ122, or TSZ124 devices for the O2 sensor application ensures that the measurement of O2 concentration is stable even at different temperature thanks to a very good $\Delta V_{io}/\Delta T$.

5.11.2 Precision instrumentation amplifier

The instrumentation amplifier uses three op amps. The circuit, shown in [Figure 48. Precision instrumentation amplifier schematic](#), exhibits high input impedance, so that the source impedance of the connected sensor has no impact on the amplification.

Figure 48. Precision instrumentation amplifier schematic


The gain is set by tuning the R_g resistor. With $R_1 = R_2$ and $R_3 = R_4$, the output is given by [Section 5.11.2 Equation 3](#).

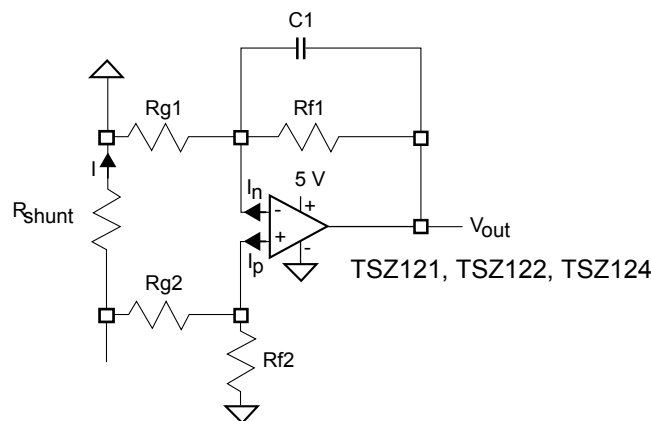
Equation 3

$$V_{out} = (V_2 - V_1) \left[\frac{R_4}{R_2} \cdot \frac{2R_f}{R_g} + 1 \right]$$

The matching of R_1 , R_2 and R_3 , R_4 is important to ensure a good common mode rejection ratio (CMR).

5.11.3
Low-side current sensing

Power management mechanisms are found in most electronic systems. Current sensing is useful for protecting applications. The low-side current sensing method consists of placing a sense resistor between the load and the circuit ground. The resulting voltage drop is amplified using TSZ121, TSZ122, and TSZ124 devices (see [Figure 49. Low-side current sensing schematic](#)).

Figure 49. Low-side current sensing schematic


V_{out} can be expressed as follows:

Equation 4

$$V_{out} = R_{shunt} \times I \left(1 - \frac{R_{g2}}{R_{g2} + R_{f2}} \right) \left(1 + \frac{R_{f1}}{R_{g1}} \right) + I_p \left(\frac{R_{g2} \times R_{f2}}{R_{g2} + R_{f2}} \right) \times \left(1 + \frac{R_{f1}}{R_{g1}} \right) - I_n \times R_{f1} - V_{io} \left(1 + \frac{R_{f1}}{R_{g1}} \right)$$

Assuming that $R_{f2} = R_{f1} = R_f$ and $R_{g2} = R_{g1} = R_g$, [Equation 4](#) can be simplified as follows:

Equation 5

$$V_{out} = R_{shunt} \times I \left(\frac{R_f}{R_g} \right) - V_{io} \left(1 + \frac{R_f}{R_g} \right) + R_f \times I_{io}$$

The main advantage of using the chopper of the TSZ121, TSZ122, and TSZ124, for a low-side current sensing, is that the errors due to V_{io} and I_{io} are extremely low and may be neglected.

Therefore, for the same accuracy, the shunt resistor can be chosen with a lower value, resulting in lower power dissipation, lower drop in the ground path, and lower cost.

Particular attention must be paid on the matching and precision of R_{g1} , R_{g2} , R_{f1} , and R_{f2} , to maximize the accuracy of the measurement.

6 Package information

In order to meet environmental requirements, ST offers these devices in different grades of **ECOPACK®** packages, depending on their level of environmental compliance. ECOPACK® specifications, grade definitions and product status are available at: www.st.com. ECOPACK® is an ST trademark.

6.1 SC70-5 (or SOT323-5) package information

Figure 50. SC70-5 (or SOT323-5) package outline

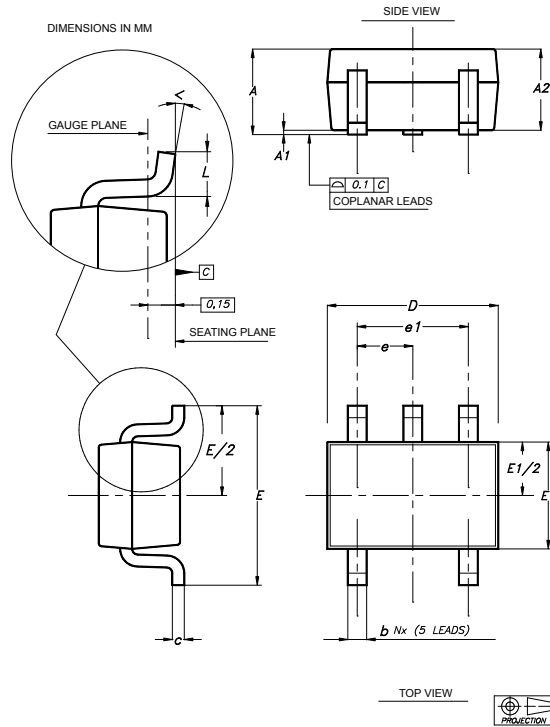


Table 6. SC70-5 (or SOT323-5) mechanical data

Ref.	Dimensions					
	Millimeters			Inches		
	Min.	Typ.	Max.	Min.	Typ.	Max.
A	0.80		1.10	0.032		0.043
A1			0.10			0.004
A2	0.80	0.90	1.00	0.032	0.035	0.039
b	0.15		0.30	0.006		0.012
c	0.10		0.22	0.004		0.009
D	1.80	2.00	2.20	0.071	0.079	0.087
E	1.80	2.10	2.40	0.071	0.083	0.094
E1	1.15	1.25	1.35	0.045	0.049	0.053
e		0.65			0.025	
e1		1.30			0.051	
L	0.26	0.36	0.46	0.010	0.014	0.018
<	0°		8°	0°		8°

6.2 SOT23-5 package information

Figure 51. SOT23-5 package outline

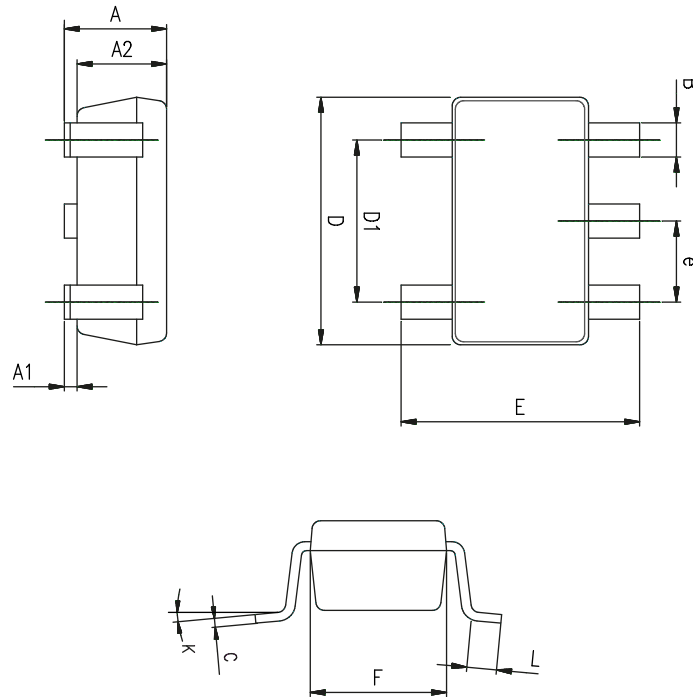


Table 7. SOT23-5 mechanical data

Ref.	Dimensions					
	Millimeters			Inches		
	Min.	Typ.	Max.	Min.	Typ.	Max.
A	0.90	1.20	1.45	0.035	0.047	0.057
A1			0.15			0.006
A2	0.90	1.05	1.30	0.035	0.041	0.051
B	0.35	0.40	0.50	0.014	0.016	0.020
C	0.09	0.15	0.20	0.004	0.006	0.008
D	2.80	2.90	3.00	0.110	0.114	0.118
D1		1.90			0.075	
e		0.95			0.037	
E	2.60	2.80	3.00	0.102	0.110	0.118
F	1.50	1.60	1.75	0.059	0.063	0.069
L	0.10	0.35	0.60	0.004	0.014	0.024
K	0 degrees		10 degrees	0 degrees		10 degrees

6.3 DFN8 2 x 2 package information

Figure 52. DFN8 2 x 2 package outline

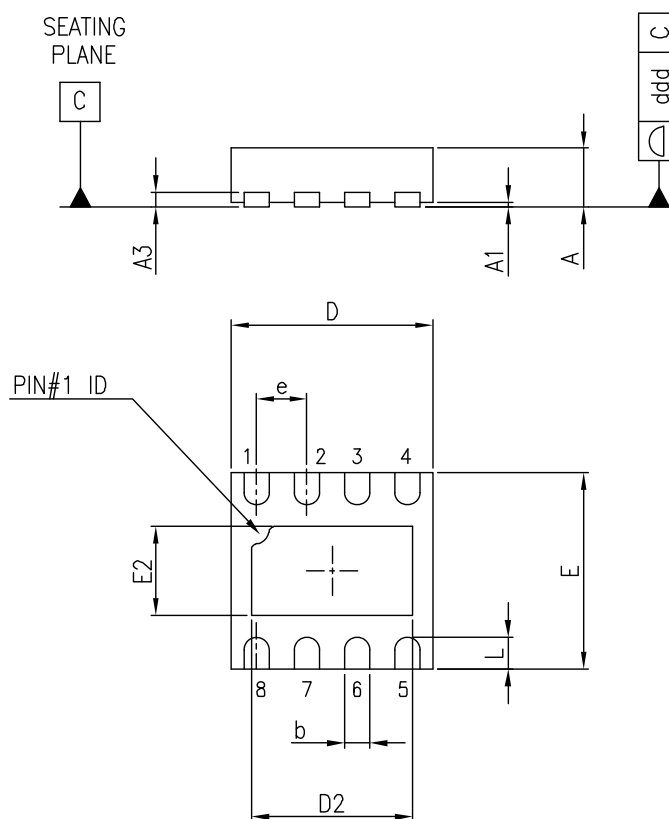
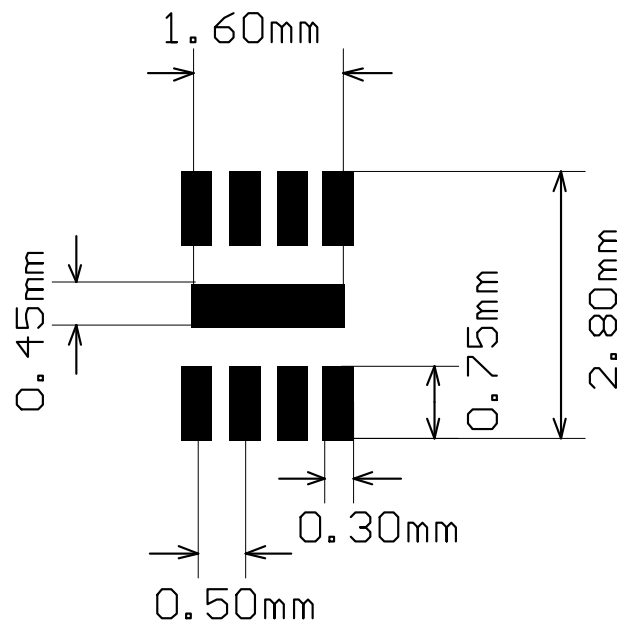


Table 8. DFN8 2 x 2 mechanical data

Ref.	Dimensions					
	Millimeters			Inches		
	Min.	Typ.	Max.	Min.	Typ.	Max.
A	0.51	0.55	0.60	0.020	0.022	0.024
A1			0.05			0.002
A3		0.15			0.006	
b	0.18	0.25	0.30	0.007	0.010	0.012
D	1.85	2.00	2.15	0.073	0.079	0.085
D2	1.45	1.60	1.70	0.057	0.063	0.067
E	1.85	2.00	2.15	0.073	0.079	0.085
E2	0.75	0.90	1.00	0.030	0.035	0.039
e		0.50			0.020	
L	0.225	0.325	0.425	0.009	0.013	0.017
ddd			0.08			0.003

Figure 53. DFN8 2 x 2 recommended footprint



6.4 MiniSO8 package information

Figure 54. MiniSO8 package outline

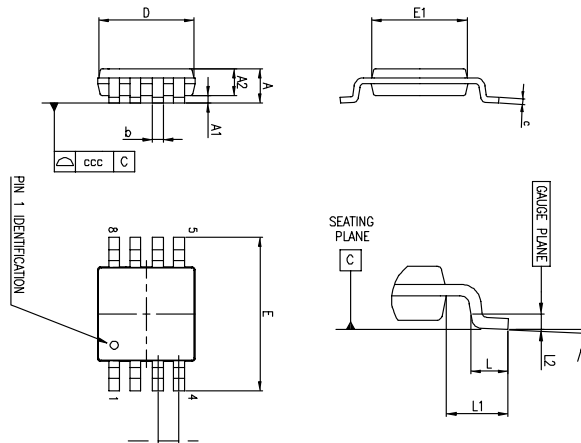


Table 9. MiniSO8 package mechanical data

Ref.	Dimensions					
	Millimeters			Inches		
	Min.	Typ.	Max.	Min.	Typ.	Max.
A			1.1			0.043
A1	0		0.15	0		0.0006
A2	0.75	0.85	0.95	0.030	0.033	0.037
b	0.22		0.40	0.009		0.016
c	0.08		0.23	0.003		0.009
D	2.80	3.00	3.20	0.11	0.118	0.126
E	4.65	4.90	5.15	0.183	0.193	0.203
E1	2.80	3.00	3.10	0.11	0.118	0.122
e		0.65			0.026	
L	0.40	0.60	0.80	0.016	0.024	0.031
L1		0.95			0.037	
L2		0.25			0.010	
k	0°		8°	0°		8°
ccc			0.10			0.004

6.5 SO8 package information

Figure 55. SO8 package outline

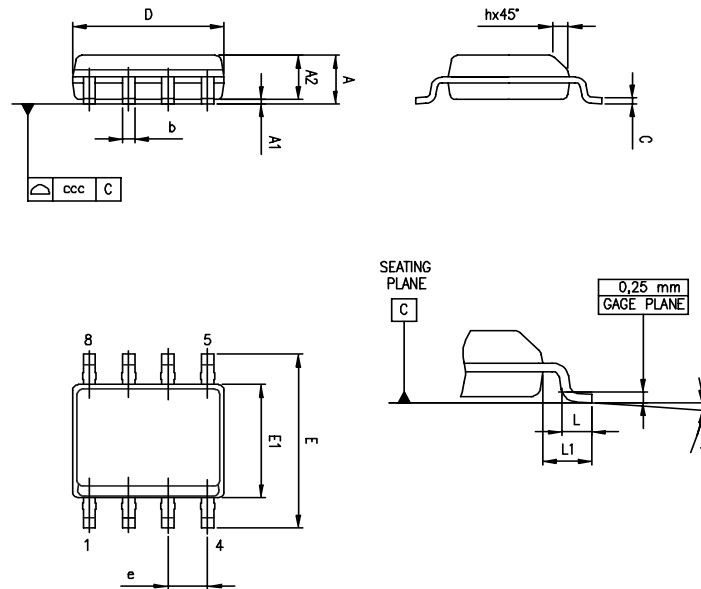


Table 10. SO8 package mechanical data

Ref.	Dimensions					
	Millimeters			Inches		
	Min.	Typ.	Max.	Min.	Typ.	Max.
A			1.75			0.069
A1	0.10		0.25	0.004		0.010
A2	1.25			0.049		
b	0.28		0.48	0.011		0.019
c	0.17		0.23	0.007		0.010
D	4.80	4.90	5.00	0.189	0.193	0.197
E	5.80	6.00	6.20	0.228	0.236	0.244
E1	3.80	3.90	4.00	0.150	0.154	0.157
e		1.27			0.050	
h	0.25		0.50	0.010		0.020
L	0.40		1.27	0.016		0.050
L1		1.04			0.040	
k	0°		8°	0°		8°
ccc			0.10			0.004

6.6 QFN16 3x3 package information

Figure 56. QFN16 3x3 package outline

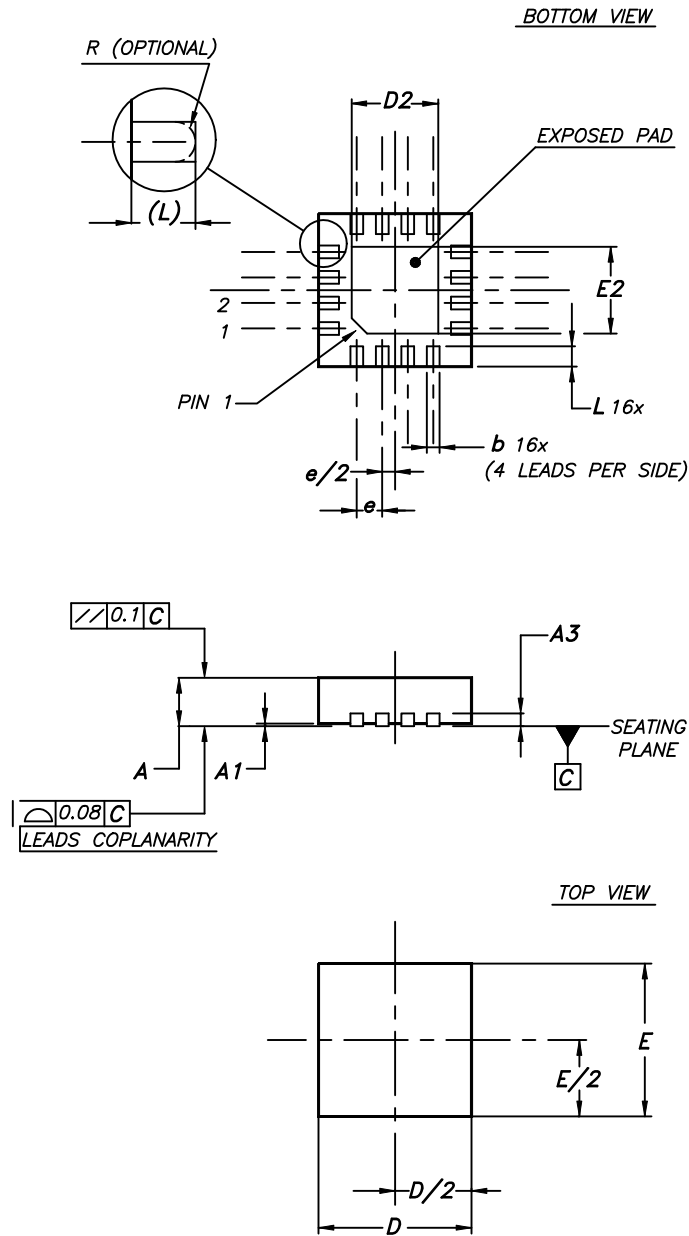
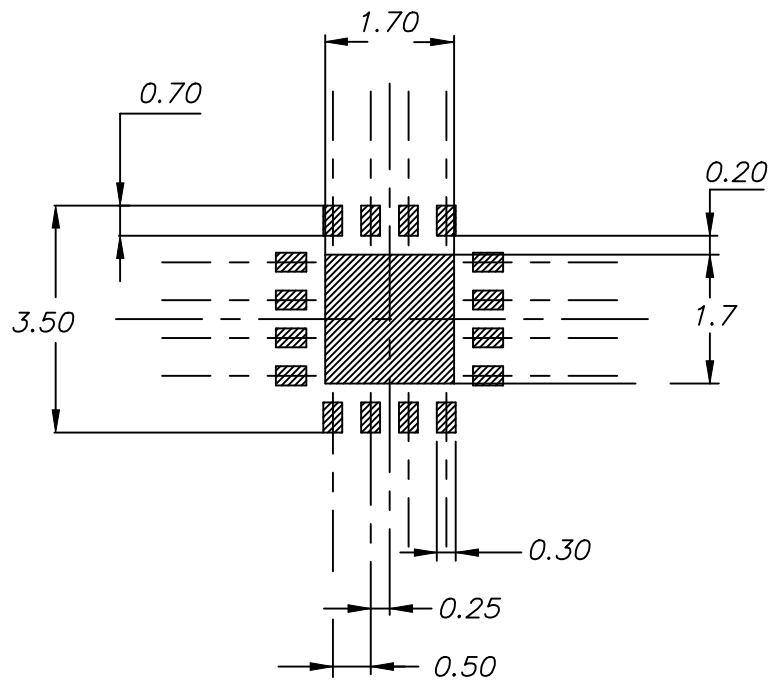


Table 11. QFN16 3x3 mechanical data

Ref.	Dimensions					
	Millimeters			Inches		
	Min.	Typ.	Max.	Min.	Typ.	Max.
A	0.80	0.90	1.00	0.031	0.035	0.039
A1	0		0.05	0		0.002
A3		0.20			0.008	
b	0.18		0.30	0.007		0.012
D	2.90	3.00	3.10	0.114	0.118	0.122
D2	1.50		1.80	0.059		0.071
E	2.90	3.00	3.10	0.114	0.118	0.122
E2	1.50		1.80	0.059		0.071
e		0.50			0.020	
L	0.30		0.50	0.012		0.020

Figure 57. QFN16 3x3 recommended footprint



6.7 TSSOP14 package information

Figure 58. TSSOP14 package outline

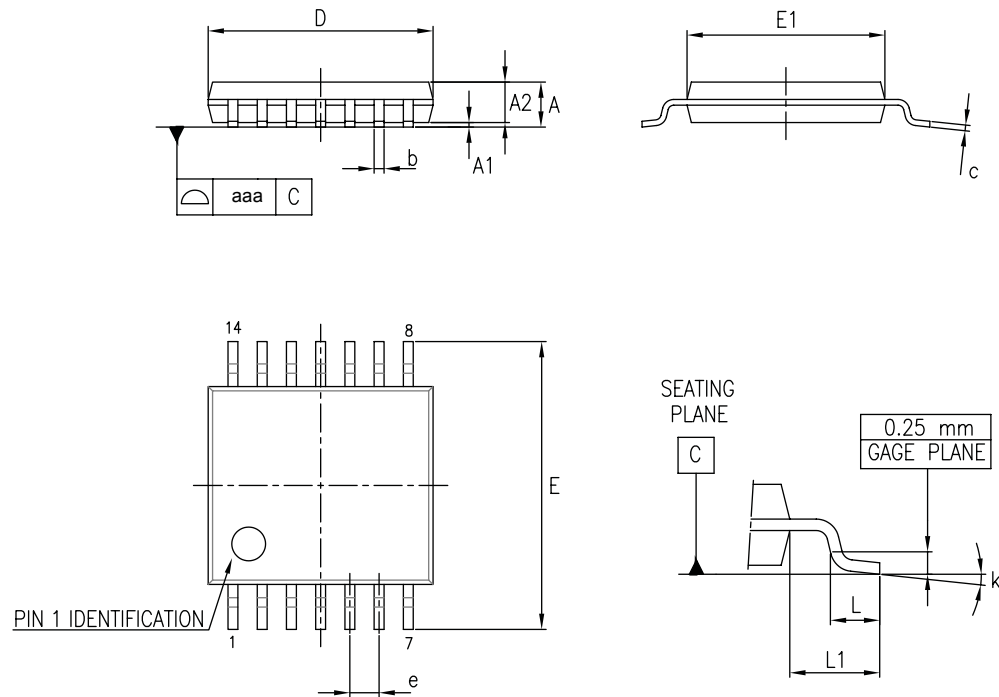


Table 12. TSSOP14 package mechanical data

Ref.	Dimensions					
	Millimeters			Inches		
	Min.	Typ.	Max.	Min.	Typ.	Max.
A			1.20			0.047
A1	0.05		0.15	0.002	0.004	0.006
A2	0.80	1.00	1.05	0.031	0.039	0.041
b	0.19		0.30	0.007		0.012
c	0.09		0.20	0.004		0.0089
D	4.90	5.00	5.10	0.193	0.197	0.201
E	6.20	6.40	6.60	0.244	0.252	0.260
E1	4.30	4.40	4.50	0.169	0.173	0.176
e		0.65			0.0256	
L	0.45	0.60	0.75	0.018	0.024	0.030
L1		1.00			0.039	
k	0°		8°	0°		8°
aaa			0.10			0.004

7 Ordering information

Table 13. Order codes

Order code	Temperature range	Package	Packaging	Marking
TSZ121ICT	-40 to 125 °C	SC70-5	Tape and reel	K44
TSZ121ILT		SOT23-5		K143
TSZ122IQ2T		DFN8 2x2		K33
TSZ122IST		MiniSO8		K208
TSZ122IDT		SO8		TSZ122I
TSZ124IQ4T		QFN16 3x3		K193
TSZ124IPT		TSSOP14		TSZ124I
TSZ121IYLT ⁽¹⁾	-40 to 125 °C automotive grade	SOT23-5		K192
TSZ122IYDT ⁽¹⁾		SO8		K192D
TSZ122IYST ⁽¹⁾		MiniSO8		K192
TSZ124IYPT ⁽¹⁾		TSSOP14		TSZ124IY

1. Qualified and characterized according to AEC Q100 and Q003 or equivalent, advanced screening according to AEC Q001 & Q002 or equivalent.

Revision history

Table 14. Document revision history

Date	Revision	Changes
16-Aug-2012	1	Initial release.
25-Apr-2013	2	Added dual and quad products (TSZ122 and TSZ124 respectively) Updated title Added following packages: DFN8 2x2, MiniSO8, QFN16 3x3, TSSOP14 Updated Features Added Benefits and Related products Updated Description Updated Table 1 (R_{thja} , ESD) Updated Table 3 (V_{io} , $\Delta V_{io}/\Delta T$, CMR, A_{vd} , I_{CC} , e_n , and C_s) Updated Table 4 (V_{io} , $\Delta V_{io}/\Delta T$, CMR, I_{CC} , e_n , and C_s) Updated Table 5 (V_{io} , $\Delta V_{io}/\Delta T$, CMR, SVR, EMIRR, I_{CC} , t_s , e_n , and C_s) Updated curves of Section 3: Electrical characteristics Added Section 4.7: Capacitive load Small update Section 4.9: Optimized application recommendation (capacitor) Added Section 4.10: EMI rejection ration (EMIRR) Updated Table 10: Order codes
11-Sep-2013	3	Added SO8 package for commercial part number TSZ122IDT Related products: added hyperlinks for TSV71x and TSV73x products Table 1: updated CDM information Figure 6, Figure 7: updated X-axes titles Figure 12: updated X-axis and Y-axis titles Figure 19: updated title Figure 26: updated X-axis (logarithmic scale) Figure 27 and Figure 28: updated Y-axis titles
23-May-2014	4	Table 1: updated ESD information Table 5: added footnote 3 Table 10: Order codes: added automotive qualification footnotes 1 and 2; updated marking of TSZ122IST. Updated disclaimer
09-May-2016	5	Updated document layout Table 13: "Order codes": added new automotive grade order code TSZ122IYD, updated footnotes of other automotive grade order codes.
07-Feb-2017	6	Table 3, Table 4, and Table 5: added parameter "Low-frequency peak-to-peak input noise" (I_{e_n}). Figure 26: "0.1 Hz to 10 Hz noise": updated legend (0.75 μV_{pp} instead of 0.2 μV_{pp})
12-Apr-2017	7	Updated footnote related to TSZ122IYDT in Table 13: "Order codes". Minor changes throughout the document.
18-May-2017	8	Updated package outline drawing and mechanical data in Section 6.2: SOT23-5 package information.
12-Nov-2018	9	Updated Figure 43. Stability criteria with a serial resistor at $V_{DD} = 5 V$ and Figure 44. Stability criteria with a serial resistor at $V_{DD} = 1.8 V$

Contents

1	Package pin connections	2
2	Absolute maximum ratings and operating conditions	3
3	Electrical characteristics	4
4	Electrical characteristic curves	8
5	Application information	14
5.1	Operation theory	14
5.1.1	Time domain	14
5.1.2	Frequency domain	15
5.2	Operating voltages	15
5.3	Input pin voltage ranges	15
5.4	Rail-to-rail input	16
5.5	Input offset voltage drift over temperature	16
5.6	Rail-to-rail output	16
5.7	Capacitive load	16
5.8	PCB layout recommendations	17
5.9	Optimized application recommendation	17
5.10	EMI rejection ration (EMIRR)	17
5.11	Application examples	18
5.11.1	Oxygen sensor	18
5.11.2	Precision instrumentation amplifier	18
5.11.3	Low-side current sensing	19
6	Package information	21
6.1	SC70-5 (or SOT323-5) package information	22
6.2	SOT23-5 package information	22
6.3	DFN8 2 x 2 package information	23
6.4	MiniSO8 package information	26
6.5	SO8 package information	26
6.6	QFN16 3x3 package information	27
6.7	TSSOP14 package information	29

7	Ordering information31
	Revision history32
	Contents33
	List of tables35
	List of figures.....	.36

List of tables

Table 1.	Absolute maximum ratings (AMR)	3
Table 2.	Operating conditions	3
Table 3.	Electrical characteristics at $V_{CC+} = 1.8\text{ V}$ with $V_{CC-} = 0\text{ V}$, $V_{icm} = V_{CC}/2$, $T = 25\text{ }^{\circ}\text{C}$, and $R_L = 10\text{ k}\Omega$ connected to $V_{CC}/2$ (unless otherwise specified)	4
Table 4.	Electrical characteristics at $V_{CC+} = 3.3\text{ V}$ with $V_{CC-} = 0\text{ V}$, $V_{icm} = V_{CC}/2$, $T = 25\text{ }^{\circ}\text{C}$, and $R_L = 10\text{ k}\Omega$ connected to $V_{CC}/2$ (unless otherwise specified)	5
Table 5.	Electrical characteristics at $V_{CC+} = 5\text{ V}$ with $V_{CC-} = 0\text{ V}$, $V_{icm} = V_{CC}/2$, $T = 25\text{ }^{\circ}\text{C}$, and $R_L = 10\text{ k}\Omega$ connected to $V_{CC}/2$ (unless otherwise specified)	6
Table 6.	SC70-5 (or SOT323-5) mechanical data	22
Table 7.	SOT23-5 mechanical data	23
Table 8.	DFN8 2 x 2 mechanical data	24
Table 9.	MiniSO8 package mechanical data	26
Table 10.	SO8 package mechanical data	27
Table 11.	QFN16 3x3 mechanical data	29
Table 12.	TSSOP14 package mechanical data	30
Table 13.	Order codes	31
Table 14.	Document revision history	32

List of figures

Figure 1.	Pin connections for each package (top view)	2
Figure 2.	Supply current vs. supply voltage	8
Figure 3.	Input offset voltage distribution at $V_{CC} = 5\text{ V}$	8
Figure 4.	Input offset voltage distribution at $V_{CC} = 3.3\text{ V}$	8
Figure 5.	Input offset voltage distribution at $V_{CC} = 1.8\text{ V}$	8
Figure 6.	V_{io} temperature co-efficient distribution ($-40\text{ }^{\circ}\text{C}$ to $25\text{ }^{\circ}\text{C}$)	8
Figure 7.	V_{io} temperature co-efficient distribution ($25\text{ }^{\circ}\text{C}$ to $125\text{ }^{\circ}\text{C}$)	8
Figure 8.	Input offset voltage vs. supply voltage	9
Figure 9.	Input offset voltage vs. input common-mode at $V_{CC} = 1.8\text{ V}$	9
Figure 10.	Input offset voltage vs. input common-mode at $V_{CC} = 2.7\text{ V}$	9
Figure 11.	Input offset voltage vs. input common-mode at $V_{CC} = 5.5\text{ V}$	9
Figure 12.	Input offset voltage vs. temperature	9
Figure 13.	V_{OH} vs. supply voltage	9
Figure 14.	V_{OL} vs. supply voltage	10
Figure 15.	Output current vs. output voltage at $V_{CC} = 1.8\text{ V}$	10
Figure 16.	Output current vs. output voltage at $V_{CC} = 5.5\text{ V}$	10
Figure 17.	Input bias current vs. common mode at $V_{CC} = 5\text{ V}$	10
Figure 18.	Input bias current vs. common mode at $V_{CC} = 1.8\text{ V}$	10
Figure 19.	Input bias current vs. temperature at $V_{CC} = 5\text{ V}$	10
Figure 20.	Bode diagram at $V_{CC} = 1.8\text{ V}$	11
Figure 21.	Bode diagram at $V_{CC} = 2.7\text{ V}$	11
Figure 22.	Bode diagram at $V_{CC} = 5.5\text{ V}$	11
Figure 23.	Open loop gain vs. frequency	11
Figure 24.	Positive slew rate vs. supply voltage	11
Figure 25.	Negative slew rate vs. supply voltage	11
Figure 26.	0.1 Hz to 10 Hz noise	12
Figure 27.	Noise vs. frequency	12
Figure 28.	Noise vs. frequency and temperature	12
Figure 29.	Output overshoot vs. load capacitance	12
Figure 30.	Small signal	12
Figure 31.	Large signal	12
Figure 32.	Positive overvoltage recovery at $V_{CC} = 1.8\text{ V}$	13
Figure 33.	Positive overvoltage recovery at $V_{CC} = 5\text{ V}$	13
Figure 34.	Negative overvoltage recovery at $V_{CC} = 1.8\text{ V}$	13
Figure 35.	Negative overvoltage recovery at $V_{CC} = 5\text{ V}$	13
Figure 36.	PSRR vs. frequency	13
Figure 37.	Output impedance vs. frequency	13
Figure 38.	Block diagram in the time domain (step 1)	14
Figure 39.	Block diagram in the time domain (step 2)	14
Figure 40.	V_{io} cancellation principle	15
Figure 41.	Block diagram in the frequency domain	15
Figure 42.	Input current limitation	16
Figure 43.	Stability criteria with a serial resistor at $V_{DD} = 5\text{ V}$	17
Figure 44.	Stability criteria with a serial resistor at $V_{DD} = 1.8\text{ V}$	17
Figure 45.	Test configuration for Riso	17
Figure 46.	EMIRR on IN+ pin	18
Figure 47.	Oxygen sensor principle schematic	18
Figure 48.	Precision instrumentation amplifier schematic	19
Figure 49.	Low-side current sensing schematic	19

Figure 50.	SC70-5 (or SOT323-5) package outline	22
Figure 51.	SOT23-5 package outline	23
Figure 52.	DFN8 2 x 2 package outline	24
Figure 53.	DFN8 2 x 2 recommended footprint	25
Figure 54.	MiniSO8 package outline	26
Figure 55.	SO8 package outline	27
Figure 56.	QFN16 3x3 package outline	28
Figure 57.	QFN16 3x3 recommended footprint	29
Figure 58.	TSSOP14 package outline	30

IMPORTANT NOTICE – PLEASE READ CAREFULLY

STMicroelectronics NV and its subsidiaries (“ST”) reserve the right to make changes, corrections, enhancements, modifications, and improvements to ST products and/or to this document at any time without notice. Purchasers should obtain the latest relevant information on ST products before placing orders. ST products are sold pursuant to ST’s terms and conditions of sale in place at the time of order acknowledgement.

Purchasers are solely responsible for the choice, selection, and use of ST products and ST assumes no liability for application assistance or the design of Purchasers’ products.

No license, express or implied, to any intellectual property right is granted by ST herein.

Resale of ST products with provisions different from the information set forth herein shall void any warranty granted by ST for such product.

ST and the ST logo are trademarks of ST. All other product or service names are the property of their respective owners.

Information in this document supersedes and replaces information previously supplied in any prior versions of this document.

© 2018 STMicroelectronics – All rights reserved